Functional model of water balance variability at the catchment scale: 1. Evidence of hydrologic similarity and space-time symmetry

Murugesu Sivapalan,[1,2,3] Mary A. Yaeger,[1] Ciaran J. Harman,[1] Xiangyu Xu,[2,4] and Peter A. Troch[5]

Received 19 May 2010; revised 8 November 2010; accepted 1 December 2010; published 16 February 2011.

[1] This paper presents analysis of annual water balance variability, (1) regional (between-catchment) variability and (2) between-year (interannual) variability and the symmetry between the two. This involved analysis of the annual water balance in terms of a two-stage partitioning, first, of annual precipitation into quick flow and soil wetting and, subsequently, of the resulting soil wetting into slow flow and vaporization. The nature of this water balance partitioning is explored by completing the above analysis in 377 Model Parameter Estimation Experiment (MOPEX) catchments located across the continental United States. We fitted analytical functional relationships to the partitioning at each stage, producing expressions for the three components of quick flow, slow flow, and vaporization. They indicate that the heterogeneity of water balance partitioning among the MOPEX catchments is underlain by a universal relationship that is transferable regionally. Key nondimensional similarity parameters are identified that serve to connect this invariant regional relationship to site-specific response characteristics. These nondimensional formulations are extended to derive analytical expressions for several common metrics of annual water balance. The ability of the functional theory to predict regional patterns of mean annual water balance and interannual variability in individual catchments is assessed. Our analyses show a close symmetry between spatial (regional) variability of mean annual water balances and general trends of temporal (interannual) variability. The suggested functional theory can thus be the basis for data-based assessments of hydrologic similarity and used to assist with predictions of the effects of long-term climate variability and change, through providing a theoretical framework for "space for time" substitutions.

Citation: Sivapalan, M., M. A. Yaeger, C. J. Harman, X. Xu, and P. A. Troch (2011), Functional model of water balance variability at the catchment scale: 1. Evidence of hydrologic similarity and space-time symmetry, *Water Resour. Res., 47*, W02522, doi:10.1029/2010WR009568.

1. Introduction

[2] Land surface hydrology involves the study of the exchanges of water and energy between the land and the atmosphere and the movement of water within and over the land surface. How space-time variability in precipitation interacts with spatial heterogeneity of soils, topography, and vegetation and is partitioned into spatiotemporal variability of runoff, evaporation, and soil moisture storage are fundamental questions that underpin hydrologic predictions of all kinds. This hydrologic partitioning is usually expressed in terms of a dynamic water balance, which can be manifested in various characteristic signatures of catchment responses representing variability at a range of time (and also space) scales [*Wagener et al.*, 2007].

[3] An important concern for sustainable water management is how climate variability and/or change at annual to decadal time scales, and likewise hydrologic effects of land use and land cover changes, propagate through the landscape and result in changes to spatiotemporal patterns of variability of water balance over a range of time and space scales. Over the past 5 decades, considerable effort has been invested into exploring the roles of climate, soil, vegetation, and topography interactions in controlling water balance variability (both in time and in space) at the annual scale in order to generate the understanding needed to make predictions of the resulting changes to the water balance. Much more effort has been expended, however, in studying mean annual water balance than on interannual variability.

[4] This paper develops a framework for analyzing the space and time variability of annual water balances. In a companion paper [*Harman et al.*, 2011], this framework is used to understand the controls on sensitivity of water balance to interannual variations in precipitation. The framework used by both papers is built on previous work by *L'vovich* [1979] and *Ponce and Shetty* [1995a, 1995b]. Here we review previous approaches to water-balance modeling in order to motivate the (re)introduction of this

[1]Department of Civil and Environmental Engineering, University of Illinois at Urbana-Champaign, Urbana, Illinois, USA.
[2]Department of Geography, University of Illinois at Urbana-Champaign, Urbana, Illinois, USA.
[3]Department of Water Management, Faculty of Civil Engineering and Geosciences, Delft University of Technology, Delft, Netherlands.
[4]Department of Hydraulic Engineering, Tsinghua University, Beijing, China.
[5]Department of Hydrology and Water Resources, University of Arizona, Tucson, Arizona, USA.

0043-1397/11/2010WR009568

framework. Past research into annual water balances has followed essentially two diametrically opposite and yet complementary approaches: empirical and process based.

1.1. Mean Annual Water Balance

[5] In the empirical approach, annual water balance is assessed on the basis of systematic analysis of long-term data sets of observed rainfall and runoff in different climatic or ecoregions of the world and empirical analyses of how the water balance is governed by climatic and landscape properties. A classic example of the empirical approach to analysis of mean annual water balance is the work of *Budyko* [1974], who viewed annual water balance, to first order, as a manifestation of the competition between available water and available energy. Budyko quantified mean annual water balance in terms of the ratio of mean annual evaporation to mean annual precipitation, E/P. On the basis of worldwide data sets from a large number of catchments, he demonstrated that E/P is determined, to first order, by the ratio of mean annual potential evaporation (i.e., measure of energy available) to mean annual precipitation (i.e., measure of water available), E_p/P, which he defined as a (climatic) aridity index. In recent times, *Zhang et al.* [2001] extended the analysis of mean annual water balances, still working within the Budyko framework, to include the effects of the conversion of native (woody) vegetation to pasture and presented empirical relationships for E/P as a function of not only E_p/P but also a parameter W, which is a coefficient that reflected plant available water. *Yang et al.* [2007] carried out theoretical studies (based on dimensional analysis) leading to the analytical derivation of the Budyko curve, implemented this theory in over 100 catchments in China, and derived expressions for E/P as a function of E_p/P, the fraction of forest cover and a measure of soil moisture storage capacity (which can be partly related to soil depth).

[6] The value of these empirical approaches is that they involved deriving simple relationships governing long-term mean annual water balance, which has emerged through coevolution and self-organization of climate, soil, topography, and vegetation in different natural settings. However, it is not clear that they are sufficient to capture the climatic and landscape controls on more transient responses, including natural interannual variability, and catchment responses to nonstationary variations of both climate and changes in landscape properties through human actions. The latter will require a combination of both process-based and empirical approaches.

[7] In the process-based approach, the mean annual water balance is explored on the basis of explicit representations of the various hydrologic processes (e.g., infiltration, storage, drainage, evaporation, and transpiration) that constitute the water balance equation and the interacting roles of climate, soil, topography, and vegetation that govern these. The best example of the process-based approach to annual water balance is the classic work of *Eagleson* [1978] and *Eagleson and Tellers* [1982], who explored the cascading of a series of precipitation events through the landscape, in terms of alternative wetting and drying cycles, and explored their manifestation as mean annual water balance. In subsequent work, *Milly* [1994a] investigated the climate-landscape interactions governing the mean annual water balance through the use of a simple stochastic bucket model and used it to explore the physical basis of the *Budyko* [1974] curve, including competition between precipitation and atmospheric demand (i.e., water and energy) and the regulating influence of soil moisture storage. *Salvucci and Entekhabi* [1995] extended the mathematical formulations of *Eagleson*'s [1978] and *Eagleson and Tellers*'s [1982] work to explore the role of lateral flow processes in hillslopes. *Reggiani et al.* [2000] explored the physical basis of annual water balance by utilizing a lumped numerical model at the hillslope scale, which involved solution of the coupled mass and momentum balance equations that underpin the partitioning of precipitation into evaporation and both surface and subsurface runoff. They found that while total annual evaporation and runoff were predominantly governed by the Budyko-type aridity index, topographic slope and soil hydraulic conductivity were important factors in the partitioning of total runoff into surface and subsurface runoff.

[8] A number of studies utilized process-based models to explicitly investigate the effects of climatic seasonality on mean annual water balance. *Milly* [1994a, 1994b] and *Potter et al.* [2005] used conceptual (bucket) models to investigate the effects of climatic seasonality, through inclusion of interactions of seasonal climatic fluctuations with soil moisture storage. In this case, the effects of topography and subsurface drainage can become important determinants of intra-annual variability of water balance, which can be expected to have significant impacts also on mean annual water balance and interannual variability. *Yokoo et al.* [2008] explored the effects of seasonal variability of climatic inputs on mean annual water balances and the roles of climate, soil properties, and topography in modulating these impacts. Their numerical experiments with the use of a physically based water balance model [*Reggiani et al.*, 2000] showed that (1) the effects of seasonality are likely to be most important when the seasonal variabilities of precipitation and potential evaporation are out of phase and in arid climates and (2) the seasonality effects can be high in catchments with fine-grained soils and flat topographies, in which case surface runoff dominates, and also high in basins with coarse-grained soils and steep topographies, where subsurface runoff dominates.

1.2. Between-Year Variability of Annual Water Balance

[9] Interannual variability of the water balance response of natural (i.e., nonhuman impacted) catchments can arise, in a straightforward manner, from interannual variability of precipitation inputs or energy inputs. If catchment ecosystems can be assumed to respond, and adapt, rapidly to such variability, one can expect that empirical models of mean annual water balance [e.g., *Budyko*, 1974] can continue to reflect such interannual variability as well. A number of authors have exploited this space-time symmetry for quantifying interannual variability of annual water balance. *Yang et al.* [2007] extended the use of the Budyko framework to predict interannual variability of runoff and demonstrated reasonable accuracy in these predictions. Indeed, they extended it even further so as to predict, with reasonable accuracy, intra-annual (monthly) variability of runoff by explicitly accounting for the carryover of soil moisture storage

between months. *Wang et al.* [2009] also adopted the Budyko framework to explore regional water balances in the Sand Dune Hills region of Nebraska and identified soil texture and groundwater as major controls on mean annual water balance and interannual variability. In a much earlier classic work, *Dooge* [1992] proposed that interannual variability of annual water balance can be predicted by working within the Budyko framework through derivation of a general expression for the elasticity of annual runoff to changes in annual precipitation or potential evaporation.

[10] However, in addition, interactions of intra-annual variability of climate inputs with the landscape processes (e.g., soil moisture storage and subsurface drainage) can also manifest in additional contributions to interannual variability. Process controls of interannual variability are therefore complex. Empirical methods based on annual water balance data alone are not sufficient to fully capture interannual variability; more process studies of intra-annual variability are therefore required to develop predictive understanding of the causes of interannual variability. *Jothityangkoon and Sivapalan* [2009], through analysis of data from a small number of catchments in Australia and New Zealand, with the use of diagnostic analysis of models of increasing complexity, highlighted the roles of intra-annual precipitation variability (seasonality versus storminess) on the interannual variability of runoff. *Potter and Zhang* [2009] confirmed the validity of these approaches using data from a large number of pristine catchments in Australia and in the process demonstrated the role of intra-annual (seasonal) variability of climate variables (precipitation and potential evaporation) on interannual variability of annual water balance. Recently, *Peel et al.* [2010] showed that differences in intra-annual variations of evapotranspiration between deciduous and evergreen vegetation types can also lead to interannual variability of runoff.

1.3. Functional Approach: Horton, L'vovich, and Ponce and Shetty

[11] Because interannual variability of annual water balance is affected significantly by intra-annual variability of climatic inputs and their interactions with the processes of soil moisture storage, plant water uptake, and subsurface drainage, analyses of interannual variability will not be complete until these catchment functions are explicitly considered. Both the empirical and process-based approaches must be generalized to account for the intra-annual variability and associated process interactions. A step forward in this direction is the work of *Horton* [1933] and of *L'vovich* [1979].

[12] As far back as 1933, Horton investigated interannual variability of water balance by exploring the capacity of catchments to store infiltrated water, as a function of soil type, and evaporate it in return, as controlled by vegetation. As part of his now classic paper, he introduced the ratio of catchment vaporization (transpiration plus evaporation) V to catchment wetting by precipitation (i.e., that part of the precipitation that does not run off immediately; this includes interception, surface ponding, and soil wetting), denoted as W. This ratio V/W (hereinafter referred to as the Horton index H [*Troch et al.*, 2009]) was found to remain remarkably constant from year to year when applied to only the growing season in a catchment located in New York (west branch of the Delaware; mean of 0.78 and standard deviation of 0.06), despite the large interannual variability of growing season precipitation (minimum of 406 mm, maximum of 812 mm). On the basis of these observations, *Horton* [1933, p. 456] hypothesized that the "natural vegetation of a region tends to develop to such an extent that it can utilize the largest possible proportion of the available soil moisture supplied by infiltration."

[13] Motivated by Horton's stated hypothesis, *Troch et al.* [2009] estimated the Horton index for 89 catchments around the continental United States and confirmed that the Horton index does, indeed, remain remarkably constant between years in these catchments, with a relatively small variance. For example, Troch et al.'s analysis showed that for 50% of the catchments analyzed, the standard deviation of the Horton index is less than 0.06, while in about 90% of the cases the standard deviation is less than 0.10. Troch et al. also showed that as the aridity index E_p/P increased, the mean Horton index also increased, while its variability decreased significantly. In addition, the marked symmetry that the observed data exhibited between regional (between-catchment) variability of the Horton index (reflecting climate variability between catchments) and interannual (between-year) variability (a reflection of interannual variability of climatic inputs) suggested to them that vegetation across different ecoregions may be adapting in very similar ways to spatiotemporal variability of water and energy availability.

[14] In this paper we adopt an extension of the Hortonian approach to interannual variability, pioneered by *L'vovich* [1979], who presented an empirical theory for the two-stage water balance partitioning at the land surface. According to this theory, in the first stage, precipitation is partitioned into wetting (of canopy, litter, and soil) and quick flow (e.g., surface runoff), whereas in the second stage the wetting is further partitioned into vaporization (interception loss plus evaporation plus transpiration) and slow flow (e.g., subsurface runoff). The original work of *L'vovich* [1979] and subsequent work by *Ponce and Shetty* [1995a, 1995b] theorized that the partitioning at each stage is in the form of a competition between different catchment functions, which are expressible in terms of common mathematical forms that can be extracted from data. *L'vovich* [1979] implemented this approach in a large number of catchments located in a variety of ecoregions of the world and presented his results in the form of nomographs. In spite of the increased global interest in annual water balances and concerns about the effects of global change, apart from the theoretical analyses of *Ponce and Shetty* [1995a, 1995b], the work of *L'vovich* [1979] has not been subsequently followed up, despite at least 40 years of additional data that have become available. The *Horton* [1933] and *L'vovich* [1979] approaches are partly empirical since they are based on empirical analyses of rainfall-runoff data for the characterization of annual water balances. On the other hand, since they go further than Budyko and explicitly include the partitioning of annual precipitation into its major components of storage, release by quick flow and slow flow, and evapotranspiration (combining bare soil evaporation, interception loss, and plant water uptake), the Horton and L'vovich approaches can be deemed to characterize the functioning of the catchments at the annual scale.

For these reasons, following *Wagener et al.* [2007], we define their approach as a *functional* approach.

1.4. Aims of This Paper

[15] This paper is aimed at exploring the variability of annual water balances, (1) regional, between-catchment variability of mean annual water balances and (2) the between-year (interannual) variability in a small number of selected catchments and the possible symmetry between these two kinds of variability, within the theoretical framework provided by the *L'vovich* [1979] and *Ponce and Shetty* [1995a, 1995b] formulations. We repeat the empirical analyses of *L'vovich* [1979] for 431 catchments in the continental United States and quantify the two-stage partitioning of precipitation at the catchment scale in all catchments. We fit the theoretical relationships of *Ponce and Shetty* [1995a, 1995b] to the resulting partitioning and explore regional patterns of the associated parameter values. Using nondimensional forms of the L'vovich–Ponce-Shetty relations, we investigate similarity of annual water balance responses between catchments and between years. In particular, we derive analytical expressions for several metrics of annual water balances: Horton index, a vaporization fraction (reflecting the Budyko curve), a base flow fraction, and a runoff fraction (equivalent to the traditional annual runoff coefficient). Finally, we use the same formulations to quantify the degree of damping of interannual variability of annual precipitation as it cascades through the catchment system and as manifested in the vaporization fraction (Budyko curve) and the Horton index to shed more light on Horton's hypothesis about the role of vegetation.

[16] The work presented in this paper complements parallel work being presented in two companion papers by S. Zanardo et al. (A stochastic, analytical model of the Horton index and implications for its physical controls, submitted to *Water Resources Research*, 2011) and H. Voepel et al. (Climate and landscape controls on catchment-scale vegetation water use, submitted to *Water Resources Research*, 2011) based on analysis of the same 431 Model Parameter Estimation Experiment (MOPEX) catchments as used in this study. Voepel et al. (submitted manuscript, 2011) adopt an empirical approach to interannual variability of annual water balances. They use rainfall-runoff data from the MOPEX catchments to develop empirical relationships between the Horton index and associated climatic and landscape properties. They also test the hypothesis that the Horton index can more reliably (than precipitation or aridity index) predict vegetation response quantified using annual maximum normalized difference vegetation index (NDVI). Zanardo et al. (submitted manuscript, 2011) adopt a process-based approach to evaluation of interannual variability and explore the climatic and landscape controls on the Horton index. For this they use a parsimonious catchment model driven by stochastic precipitation inputs, following the work of *Milly* [1994a, 1994b], *Porporato et al.* [2004], and *Botter et al.* [2007]. In this sense, the present paper and those of Voepel et al. (submitted manuscript, 2011) and Zanardo et al. (submitted manuscript, 2011) represent three alternative perspectives on the nature of annual water balance variability, both regional and interannual. Furthermore, another companion paper by *Harman et al.* [2011] adopts the same functional approach but extends the analysis to include the sensitivity and possible resilience of regional and interannual variability of water balance to changes in the climate drivers, in this case annual precipitation.

[17] The paper begins, in section 2, with a presentation of the *L'vovich* [1979] theory and the analytical formulations of *Ponce and Shetty* [1995a, 1995b]. Section 3 presents the empirical water balance analysis of the 431 MOPEX catchments to quantify the two-stage partitioning of annual precipitation into its three components, the fitting of the Ponce-Shetty functional forms to these empirical relationships, and the estimation of the associated parameters. Section 4 reformulates the Ponce and Shetty relationships into nondimensional forms in order to compactly represent the idea of "competition" and the possible symmetry between interannual and intercatchment variability and to assess these through analysis of the MOPEX data set. Section 5 uses this nondimensional formulation to derive analytical expressions for several metrics of annual water balance, including the Horton index, the vaporization fraction, and the base flow fraction, to demonstrate the unity of these formulations for characterizing between-catchment and between-year variability of annual water balance. Section 6 presents and implements the theory governing propagation of interannual variability through the catchment system and a quantification of the damping of variability produced during the two-stage partitioning. Finally, the paper concludes with a discussion of the results, their implications, and recommendations for further research.

2. Water Balance Partitioning at Annual Scale: L'vovich and Ponce and Shetty Theories

2.1. L'vovich Theory

[18] *L'vovich* [1979] presented an empirical theory of annual water balance that is based on a two-stage partitioning of annual precipitation into three components: quick flow, slow flow, and vaporization, as illustrated in Figure 1.

[19] At the first stage, precipitation P is partitioned into a quick flow component S and an infiltrated component called catchment wetting W. At the second stage, the resulting catchment wetting W is then further partitioned into a slow-flow component U and an energy-dependent

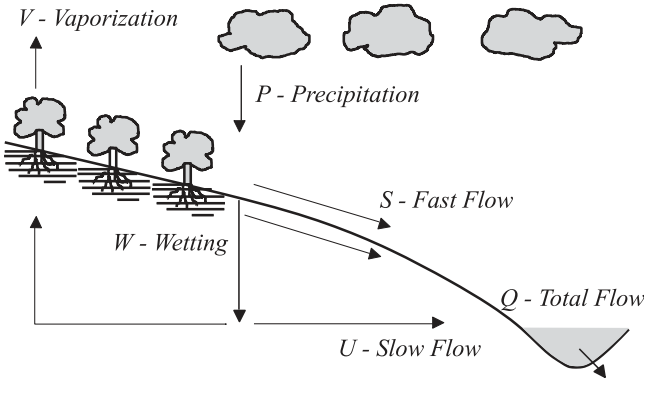

Figure 1. Conceptual model of the water balance partitioning at the land surface according to *L'vovich* [1979]. After *Ponce and Shetty* [1995a].

vaporization component (evaporation plus transpiration) V. Both the quick-flow and slow-flow components combine together to yield the total discharge Q in the stream.

[20] This two-stage hydrologic partitioning can be mathematically represented as follows:

$$P = S + W, \tag{1}$$

$$W = U + V. \tag{2}$$

[21] The combined annual water balance, neglecting carryover of storage between consecutive years, can then be written as

$$P = V + Q, \tag{3}$$

$$Q = S + U. \tag{4}$$

[22] *L'vovich* [1979] implemented this theory in a large number of catchments in most ecoregions of the world. This was done by assembling continuous data on precipitation and streamflow and then applying a base flow separation procedure to partition total streamflow into a slow-flow (e.g., base flow) component and a quick-flow (e.g., surface flow) component. Aggregating all quantities to the annual scale, he was then able to estimate, P, Q, S, and U for every year of record, then, through differencing, W and V.

[23] Once the partitioning was completed, *L'vovich* [1979] then estimated empirical relationships for S versus P and W versus P for the first-stage partitioning and U versus W and V versus W for the second-stage partitioning. He presented the results in the form of nomographs and tables and highlighted regional differences in these relationships between the different ecoregions of the world.

[24] In spite of the differences, the empirical relationships exhibited some common, universal patterns, shown schematically in Figure 2. At the first-stage partitioning, there appears to be a threshold value of annual precipitation that must be satisfied before there is any quick flow; all precipitation up to this threshold goes into catchment wetting (of canopy, surface, and soil). On the other hand, there appears to be an upper limit to the wetting (i.e., the volume of rainfall that enters the soil). With increasing precipitation the wetting approaches this upper limit, and as it does, progressively less of the precipitation goes into wetting, and more goes into quick flow. In the asymptotic limit, quick flow grows at the same rate as precipitation.

[25] Interestingly, the empirical analyses of *L'vovich* [1979] revealed an identical situation for the second-stage partitioning of soil wetting W into vaporization V and slow flow U, as shown in Figure 2. Once again, there appears to be a threshold value of wetting that must be satisfied before there is any slow flow; all wetting up to this threshold goes into vaporization (e.g., interception loss). Again, there appears to be an upper limit to the vaporization (i.e., the volume of water that is returned to the atmosphere in vapor form). With increasing wetting, vaporization approaches this upper limit, and as it does, progressively less of the wetting goes into vaporization, and more goes into slow flow. In the limit, as before, slow flow grows at the same rate as wetting.

[26] The nature of this empirically observed partitioning suggests that with the increase of annual precipitation, control is transferred from storage (wetting) to quick flow, and with increase of wetting, control is transferred from interception and plant water use (vaporization) to subsurface drainage (slow flow). The precise role of these kinds of partitioning toward the functioning of the catchment, and the role of climate and landscape properties in it, remains to be explored.

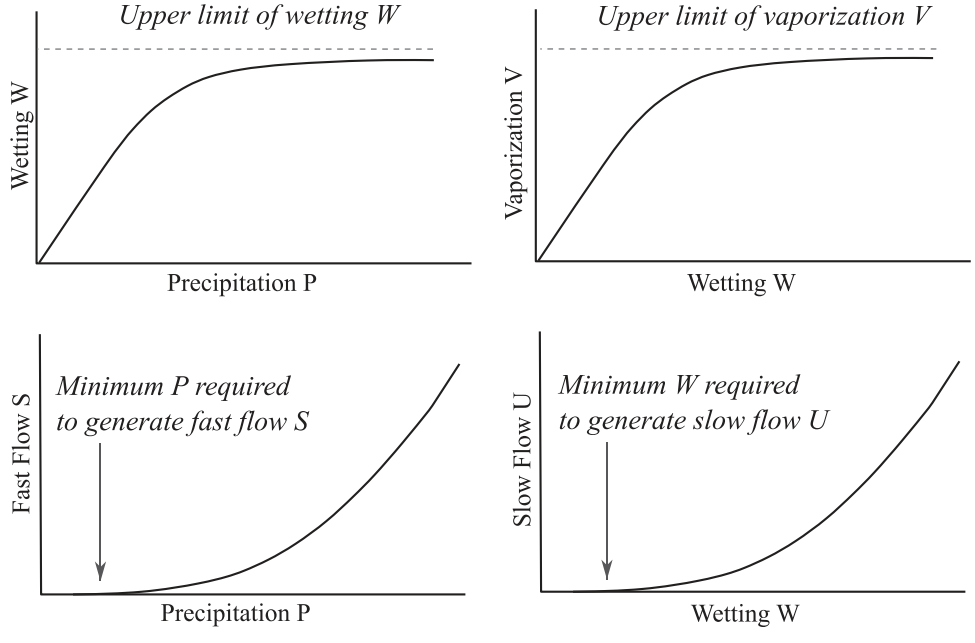

Figure 2. L'vovich-type curves illustrating precipitation partitioning. (left) Precipitation is partitioned into catchment wetting (W) and quick flow (S), and (right) wetting is partitioned into vaporization (V) and slow flow (U).

2.2. Ponce and Shetty Theory

[27] *Ponce and Shetty* [1995a, 1995b] have presented further mathematical analysis of the empirical relationships previously published by *L'vovich* [1979]. Inspired by the similarity of the S versus P and U versus W relationships to the (event-scale) Q versus P relationship in the widely used Soil Conservation Service curve number runoff generation model [*Soil Conservation Service*, 1985], *Ponce and Shetty* [1995a] postulated the following pair of mathematical models of the first-stage and second-stage partitioning. In stage 1 partitioning, $P = S + W$:

$$P < \lambda_s W_p, \quad S = 0, W = P, \tag{5a}$$

$$P > \lambda W_p, \quad S = \frac{(P - \lambda_s W_p)^2}{P + (1 - 2\lambda_s)W_p}, \qquad W = P - \frac{(P - \lambda_s W_p)^2}{P + (1 - 2\lambda_s)W_p}, \tag{5b}$$

$$P \to \infty, \quad S \to P - W_p, \quad W \to W_p. \tag{5c}$$

[28] In stage 2 partitioning, $W = U + V$:

$$W < \lambda_u V_p, \quad U = 0, \quad V = W, \tag{6a}$$

$$W > \lambda_u V_p, \quad U = \frac{(W - \lambda_u V_p)^2}{W + (1 - 2\lambda_u)V_p}, \qquad V = W - \frac{(W - \lambda_u V_p)^2}{W + (1 - 2\lambda_u)V_p}, \tag{6b}$$

$$W \to \infty, \quad U \to W - V_p, \quad V \to V_p. \tag{6c}$$

[29] The functional forms suggested in (5) and (6) can be shown to capture the general trends postulated by *L'vovich* [1979], as reproduced in Figure 2. Clearly, these are purely mathematical constructs guided by the empirical data analysis. Guided by additional physical insights and process understanding, other mathematical forms could be adopted for these relationships; this is left for further research.

[30] In equations (5) and (6), the parameters W_p and V_p are the upper bounds on W and V, which are termed as the wetting and vaporization potentials of a catchment, respectively. Meanwhile, the threshold values of P and W that must be exceeded before any flow (quick flow and slow flow, respectively) can occur are defined as $\lambda_s W_p$ and $\lambda_u V_p$, where λ_s is an abstraction coefficient associated with quick flow and λ_u is the abstraction coefficient for slow flow, with the requirement that $0 < \lambda_s, \lambda_u < 1$. In reality λ_s and λ_u will be expected to be much smaller than 1.

3. Application of the L'vovich and Ponce and Shetty Theories to MOPEX Catchments

[31] The first aim of the present study is to validate the L'vovich theory using independent and high-quality data. To this end, long-term (50 years) daily records of precipitation, streamflow, and evaporation from 431 MOPEX catchments [*Duan et al.*, 2006; see also http://www.nws.noaa.gov/oh/mopex] located across the continental United States are used, belonging to different ecoregions, with the climatic aridity index E_p/P spanning a wide range of values from 0.28 to 4.04. The drainage areas of the catchments vary between 67 and 10,329 km^2, and the data set is limited to catchments where interbasin groundwater flows are negligible. Potential evaporation climatology for these catchments is available from NOAA's free water evaporation atlas [*Farnsworth et al.*, 1982].

[32] The two-stage partitioning associated with the L'vovich theory requires, fundamentally, a separation of the total streamflow into quick flow and slow flow (e.g., base flow). The one-parameter low-pass filter developed by *Lyne and Hollick* [1979] was used here to partition the streamflow into two components, slow flow and quick flow. The value of the single filter parameter was set at 0.925 for all catchments to allow for intercomparison [see also *Arnold and Allen*, 1999; *Eckhardt*, 2005]. Initial screening of 33 catchments [*Troch et al.*, 2009] demonstrated that the estimation of annual water balance metrics, such as the Horton index, was not highly sensitive to the method of base flow separation. Figure 3 presents an example of the base flow separation obtained for one of the study catchments for one year of record. This was repeated for all 431 catchments, following which the annual aggregate values of S, W, U, and V were estimated for each year of record (note that the year here refers to the hydrological year). These annual values then formed the basis of subsequent analyses.

[33] Figure 4 presents an example of the empirical relationships obtained at the end of the base flow separation analysis. The four constituent relationships confirm the overall patterns previously obtained by *L'vovich* [1979]. Two features can be highlighted about these relationships. First, there is considerable scatter or interannual variability in these relationships, especially in the cases of the S versus P and U versus W curves, which could be due to the effects of intra-annual (within-year) variability of climatic inputs and also could be due to possible carryover of storage between years. Second, even in the case of the good result shown in Figure 4, the W versus P and V versus W relationships do not unambiguously prove the existence of an upper limit, although in the majority of cases the slopes of

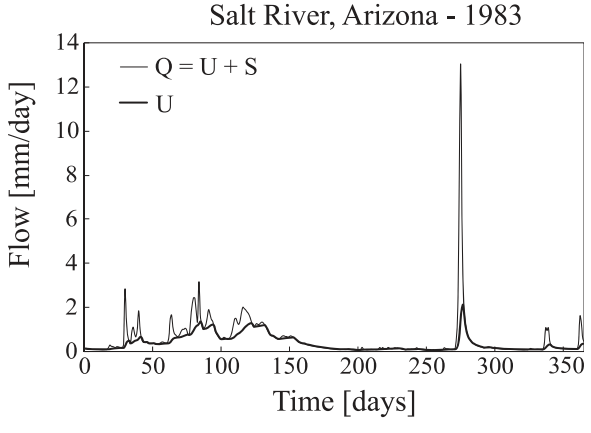

Figure 3. Separation of total streamflow into quick flow and base flow, using the *Lyne and Hollick* [1979] base flow separation procedure.

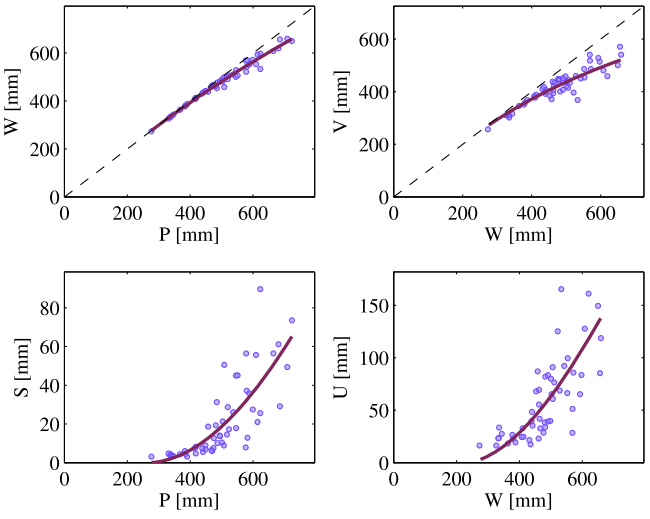

Figure 4. L'vovich relationships extracted from actual data through base flow separation (site 43, Arizona).

the curves decrease with increasing P or W. This has implications for the estimation of the four parameters, as discussed below.

[34] Upon completion of the water balance partitioning and the estimation of the empirical relationships of the type presented in Figure 4, we next set out to fit the *Ponce and Shetty* [1995a] analytical expressions and the estimation of the four parameters: W_p, V_p, λ_s, and λ_u. In the case of the first-stage partitioning, this fitting is accomplished by varying both W_p and λ_s to minimize the root-mean-square error (RMSE) of the differences between the S extracted from the runoff hydrographs and S calculated with the Ponce and Shetty model. This method is repeated for U using the values of W found from $W_{\text{calc}} = P_{\text{obs}} - S_{\text{calc}}$ to estimate the optimal values of V_p and λ_u. It would also be reasonable to fit the second-stage partitioning parameters to W_{obs} directly. We chose to use the former approach in order to obtain an internally consistent parameter set. One of the requirements of fitting a functional model to catchment data is that the range of catchment variability must exhibit the functional behavior. In this case, the wetting and vaporization potentials of a small subset of the 431 catchments could not be well identified. Some of the values of W_p and V_p obtained in this way were very much larger than the values presented by *Ponce and Shetty* [1995a], which varied from about 700 to 6000mm. A sensitivity analysis was performed to determine if these large values had any effect on model fit. The sensitivity of the fit to the parameters was calculated as $\Delta\varepsilon_s / \Delta W_p$, where ε_s is the change in RMSE of S for a small change in W_p (ΔW_p) around the calibrated value. A similar procedure was used to estimate the sensitivity of the fit for U to V_p. The results (not presented here for reasons of brevity) show that the fit is, indeed, insensitive to these extremely large values. Indeed, the data in these places do not reveal the presence of an upper limit; rather, the partitioning appears to be more or less linear. On the basis of these sensitivity analyses we identified 54 catchments where the absolute values of the sensitivity of the error in either S or U, i.e., $\Delta\varepsilon_s / \Delta W_p$, or $\Delta\varepsilon_u / \Delta V_p$, to a change in W_p or V_p, respectively, was below a set threshold value of 0.0001. We therefore excluded these 54 catchments from the scaling analyses that form the bulk of the rest of the paper because these analyses depend on the identifiability of the two upper limits, W_p and V_p. However, they are included in the more rigorous parameter identification reported in the companion paper by *Harman et al.* [2011].

[35] For illustration, the parameter values W_p, V_p, λ_s, and λ_u for 12 catchments strategically selected and belonging to different ecoregions across the United States are reproduced in Table 1. The exact locations of the selected catchments are presented in Figure 5. The data from these 12 catchments will later be used to explore the ability of the L'vovich and Ponce and Shetty theories to reproduce the interannual variability of water balance responses.

[36] The parameter values W_p (wetting potential), V_p (vaporization potential), $\lambda_s W_p$ (threshold value of P for quick flow), and $\lambda_u V_p$ (threshold value of W for slow flow) estimated for the remaining 377 MOPEX catchments are plotted over the geographical United States, displaying interesting spatial patterns, as shown in Figure 6. The mountainous Appalachian region located in the eastern United States exhibits consistently low values for all four parameters. The central (Great Plains) portion of the country exhibits large values of

Table 1. Locations, Climate Characteristics, and Ponce and Shetty Parameter Values for 12 Selected Catchments Across the United States[a]

Site	State	Region	Mean E_p (mm)	Mean P (mm)	Mean E_p/P	W_p (mm)	V_p (mm)	λ_s	λ_u	$\tilde{P}$	$\tilde{V}$	RMSE (mm)			
												S	W	U	V
142	New Hampshire	Northeast	708	1401	0.51	5261	902	0.02	0.07	0.25	0.16	41.1	41.1	70.5	101.5
271	New York	Northeast	663	1184	0.56	5019	945	0.02	0.09	0.22	0.18	25.6	25.6	62.4	78.6
392	Washington	Northwest	659	1882	0.35	10,600	1060	0.00	0.00	0.18	0.10	43.0	43.0	105.6	115.1
83	Oregon	Northwest	850	1057	0.80	8650	1321	0.02	0.00	0.11	0.16	20.0	20.0	58.3	72.9
69	West Virginia	Appalachia	716	952	0.75	3227	982	0.07	0.25	0.24	0.25	26.5	26.5	40.3	60.8
272	Virginia	Appalachia	773	960	0.81	4923	1118	0.04	0.20	0.16	0.19	23.1	23.1	45.0	64.7
138	Iowa	Midwest	998	780	1.28	3229	945	0.12	0.45	0.14	0.18	22.2	22.2	58.8	77.2
265	Kansas	Midwest	1350	760	1.78	3688	4469	0.09	0.07	0.12	1.25	23.3	23.3	18.0	40.5
46	Georgia	Southeast	866	1441	0.60	7081	1616	0.03	0.16	0.18	0.20	33.2	33.2	66.6	90.0
353	Florida	Southeast	1214	1285	0.95	8835	2580	0.06	0.21	0.09	0.25	20.5	20.5	56.3	72.5
43	Arizona	Southwest	1147	500	2.29	3065	1180	0.09	0.19	0.08	0.34	12.4	12.4	20.9	32.3
157	Texas	Southwest	1511	788	1.92	4812	4923	0.08	0.08	0.09	1.03	30.9	30.9	23.7	52.7

[a]The last four columns represent root-mean-square errors (RMSE) during the model fitting.

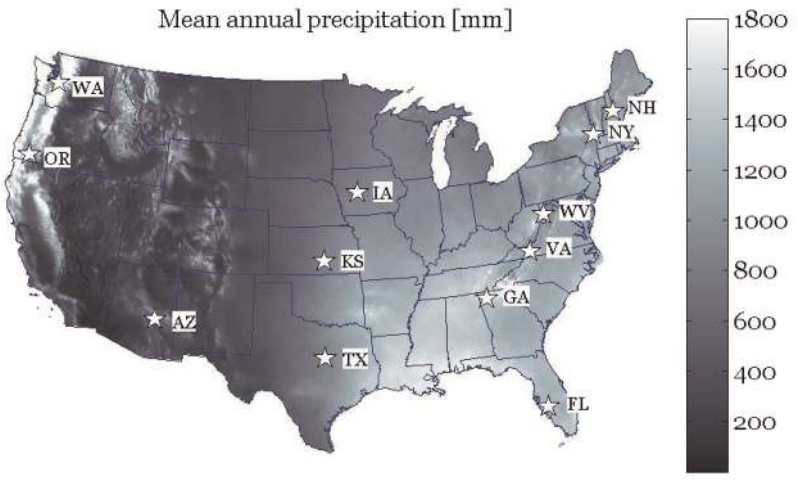

Figure 5. Locations of 12 selected catchments in different ecoregions across various levels of annual precipitation in the United States. Precipitation data were taken from http://www.prismclimate.org.

both $\lambda_s W_p$ and $\lambda_u V_p$, low W_p, and relatively high V_p. Catchments in the western United States exhibit consistently low threshold values $\lambda_s W_p$ and $\lambda_u V_p$, high values of W_p, and low values of V_p. The highest values of the threshold values $\lambda_s W_p$ and $\lambda_u V_p$ are seen in the southern (e.g., Texas) and southeastern regions (e.g., Florida) of the country. Of interest as well is the location of the 54 catchments removed from the study, as the majority of these lie to the west of the midwestern United States (Figure 6). Investigation of the physical cause of these patterns, in terms of more readily observable climatic and landscape properties, was not undertaken in this study and is left for future research. This analysis is essential if the functional theory presented here is going to be used to extrapolate to ungauged catchments.

4. Nondimensional Form of Ponce and Shetty Theory

[37] The results presented in section 3 showed substantial spatial heterogeneity in the annual water balance partitioning among the 377 MOPEX catchments. Is there an organizing principle that underpins such heterogeneous responses? How can we extract a general relationship from the site specific water balance responses? In this section we

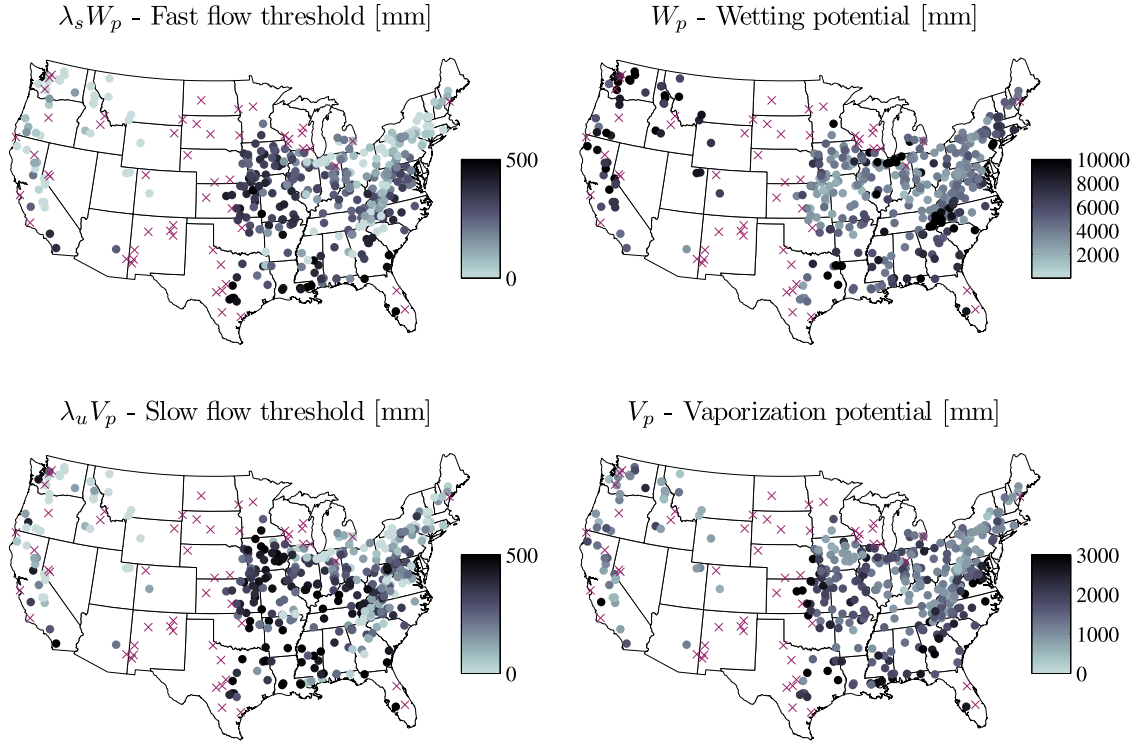

Figure 6. (left) Threshold values $\lambda_s W_p$ and $\lambda_u V_p$ and (right) potentials W_p and V_p of soil wetting W and vaporization V. The crosses represent the 54 catchments not used in the rest of the analysis.

rewrite the *Ponce and Shetty* [1995a, 1995b] formulations in nondimensional form, motivated by the expectation that this will lead to a more compact formulation, which may reveal general functional relationships common to the behavior of all the catchments, in space and in time.

[38] Consider the case $P > \lambda_s W_p$. In this case, the rainfall excess $P - \lambda_s W_p$ can be partitioned into quick flow and "excess wetting" $W - \lambda_s W_p$ as

$$(P - \lambda_s W_p) = S + (W - \lambda_s W_p). \tag{7}$$

[39] Now consider the case $W > \lambda_u V_p$. In this case the wetting excess $W - \lambda_u V_p$ can be partitioned into slow flow U and "excess" vaporization $V - \lambda_u V_p$ as follows:

$$(W - \lambda_u V_p) = U + (V - \lambda_u V_p). \tag{8}$$

[40] Using these relationships, equations (5b) and (6b) can be rearranged as follows:

$$\frac{S}{(P - \lambda_s W_p)} = \frac{(W - \lambda_s W_p)}{(1 - \lambda_s) W_p}, \tag{9a}$$

$$\frac{U}{(W - \lambda_u V_p)} = \frac{(V - \lambda_u V_p)}{(1 - \lambda_u) V_p}. \tag{9b}$$

[41] These relationships suggest that the fraction of precipitation excess that goes into quick flow is governed by the ratio of excess wetting to an upper limit $(1 - \lambda_s) W_p$. Likewise, the fraction of excess wetting that goes into slow flow is governed by the ratio of excess vaporization to its upper limit $(1 - \lambda_s) V_p$. On the basis of these observations, *L'vovich* [1979], and subsequently *Ponce and Shetty* [1995a, 1995b], theorized that the annual water balance partitioning at each stage represents a competition between two catchment functions: (1) storage versus quick flow (e.g., surface runoff) at the first stage and (2) vaporization versus slow flow (e.g., subsurface drainage) at the second stage. These ideas subsequently led to the idea of catchment functioning, as enunciated also by *Black* [1997] and later picked up by *Wagener et al.* [2007, 2008]. For these reasons, the empirical model of *L'vovich* [1979] and its extension by *Ponce and Shetty* [1995a, 1995b] can form the basis of a potentially new functional theory of annual water balance. Note that the physical basis of the competition has been previously explored by *Reggiani et al.* [2000] and *Yokoo et al.* [2008], although considerable work remains to be done to explore it from an ecohydrological perspective, considering the important role of plant water uptake and vegetation response in natural landscapes.

[42] On the basis of these considerations, we present a reformulation of the *Ponce and Shetty* [1995a, 1995b] theory in nondimensional form. As a first step, we define the following nondimensional fluxes, which represent the two-stage partitioning of precipitation:

$$S^* = \frac{S}{P - \lambda_s W_p}, \; W^* = \frac{W - \lambda_s W_p}{P - \lambda_s W_p}, \tag{10}$$

$$U^* = \frac{U}{W - \lambda_u V_p}, \; V^* = \frac{V - \lambda_u V_p}{W - \lambda_u V_p}. \tag{11}$$

[43] In addition, we define the following "driving" variables:

$$\tilde{P} = \frac{P - \lambda_s W_p}{(1 - \lambda_s) W_p}, \; \tilde{V} = \frac{V_p - \lambda_u V_p}{(1 - \lambda_s) W_p}, \; \tilde{W} = \frac{W - \lambda_u V_p}{(1 - \lambda_u) V_p}. \tag{12}$$

[44] In equation (12), $\tilde{P}$ is a rescaled annual precipitation, $\tilde{W}$ is a rescaled annual soil wetting, and $\tilde{V}$ is a rescaled vaporization limit; the latter may be deemed notionally equivalent to the concept of potential evaporation E_p. The exact relationship between E_p and $\tilde{V}$ is related to the upscaling of the water balance response from small to large space and time scales. It is clear that this upscaling does not just depend on the temporal and spatial average of energy availability that E_p typically characterizes, but rather, $\tilde{V}$ emerges from the interactions of energy and water availability with landscape structure. Elucidation of the climatic and landscape factors behind this emergent property is beyond the scope of this paper but is partially addressed by S. E. Thompson et al. (Scaling of ecologically mediated water balance partitioning: A synthesis framework for catchment ecohydrology, submitted to *Water Resources Research*, 2010). In this paper, $\tilde{V}$ is estimated from analysis of the rainfall-runoff data, although in future work its potential connection to E_p and other landscape properties may be exploited to estimate it a priori without recourse to rainfall-runoff data.

[45] We will also define a new dimensionless coefficient K, which is a function of all the four Ponce-Shetty parameters:

$$K = \frac{\lambda_s W_p - \lambda_u V_p}{(1 - \lambda_s) W_p}, \tag{13}$$

which enables $\tilde{W}$ to be rewritten as

$$\tilde{W} = \frac{K + \tilde{P} + K\tilde{P}}{\tilde{V} + \tilde{P}\tilde{V}}. \tag{14}$$

[46] One can infer from the form of equation (13) that the magnitude of K would be rather small, as will be shown later in this section. With these definitions in place, we are now in a position to rewrite the Ponce and Shetty partitioning equations in dimensionless form:

$$S^* = \frac{\tilde{P}}{1 + \tilde{P}}, \; W^* = \frac{1}{1 + \tilde{P}}, \tag{15}$$

$$U^* = \frac{\tilde{W}}{1 + \tilde{W}}, \; V^* = \frac{1}{1 + \tilde{W}}. \tag{16}$$

[47] Even though the nondimensional formulations were derived for the cases $P > \lambda_s W_p$ and $W > \lambda_u V_p$ only, they are nevertheless valid for $P < \lambda_s W_p$ and $W < \lambda_u V_p$ as well in the sense that in the case $P < \lambda_s W_p$, $S^* = 0$ and $W^* = 1$ and, similarly, in the case $W < \lambda_u V_p$, $U^* = 0$ and $V^* = 1$. Taken together, these formulations satisfy the condition that

$$S^* + W^* = 1, \; U^* + V^* = 1, \tag{17}$$

which reflects the notion of a competition between S and W in the first-stage partitioning and between U and V in the second-stage partitioning. A remarkable feature of equations (15) and (16) is that the resulting nondimensionalized relationships are parameter free (i.e., no additional parameters). In this sense, they represent universal behavior that may be deemed to connect heterogeneous site-specific responses, with the caveat that this is partially a result of the functional forms adopted by *Ponce and Shetty* [1995a].

[48] Figure 7a presents an illustration of the nature of this competition using estimates of S^*, W^*, U^*, and V^* based on mean annual estimates of S, W, U, and V for 377 MOPEX catchments. The same analysis can also be performed using rainfall and runoff data for all years (thus capturing their interannual variability) to assess the adequacy of Ponce and Shetty theory to predict the water balance partitioning in individual years. Figure 7b presents these results for the 12 catchments selected in different ecoregions highlighted in Table 1 and Figure 5. The results confirm that the same trends seen in the variability in mean annual water balance between catchments (Figure 7a) are also manifested in the variability of annual water balance between years (Figure 7b), highlighting a remarkable symmetry between spatial (regional) and temporal (interannual) variability. This will be pursued further in section 5.

5. Space-Time Variability of Annual Water Balances: Similarity Analysis

[49] Having established the L'vovich and Ponce and Shetty formulations of water balance partitioning in the MOPEX catchments, we next explore their manifestation in several alternative and classic metrics of the water balance variability at the annual scale, including interannual variability, defined below. Using the L'vovich–Ponce-Shetty notation, these metrics can be defined as

$$\begin{aligned} \textit{Horton Index} &= \frac{V}{W}, \textit{Baseflow Fraction} = \frac{U}{P}, \\ \textit{Vaporization Fraction} &= \frac{V}{P}, \textit{Runoff Fraction} = \frac{U+S}{P}. \end{aligned} \tag{18}$$

[50] The Horton index was originally introduced by *Horton* [1933], the analysis of which was extended by *Troch et al.* [2009]. The vaporization fraction is the same as E/P used by *Budyko* [1974]. The runoff fraction is the same as the annual runoff coefficient widely used by several authors. The base flow fraction we use here, which is the ratio of U to P, is different from the base flow index commonly used in the literature, i.e., the ratio of U to $(U + S)$. Note that the runoff fraction is complementary to the vaporization fraction (i.e., 1 − Vaporization Fraction).

5.1. Nondimensional Formulation of Annual Water Balance Metrics

[51] We use the nondimensional *Ponce and Shetty* [1995a, 1995b] model formulation presented in section 4 to derive analytical expressions for each of the above four water balance metrics as the means to develop compact representations of annual water balance variability. In order to recognize common links between the metrics, we define the following nondimensional variables:

$$\begin{aligned} K_H &= \frac{V - \lambda_u V_p}{W - \lambda_u V_p}, \; K_B = \frac{U}{P - \lambda_u V_p}, \\ K_V &= \frac{V - \lambda_u V_p}{P - \lambda_u V_p}, \; K_R = \frac{S + U}{P - \lambda_u V_p}. \end{aligned} \tag{19}$$

[52] This makes them slightly different from classic metrics found in the literature (e.g., Budyko curve, base flow index, and runoff coefficient). On the basis of the definitions given above, we can see that

[53] Horton index

$$K_H = V^*, \tag{20}$$

[54] Base flow fraction

$$K_B = \frac{U^*}{\left(1 + \frac{K}{\tilde{P}}\right)} \left(\frac{K}{\tilde{P}} + W^*\right), \tag{21}$$

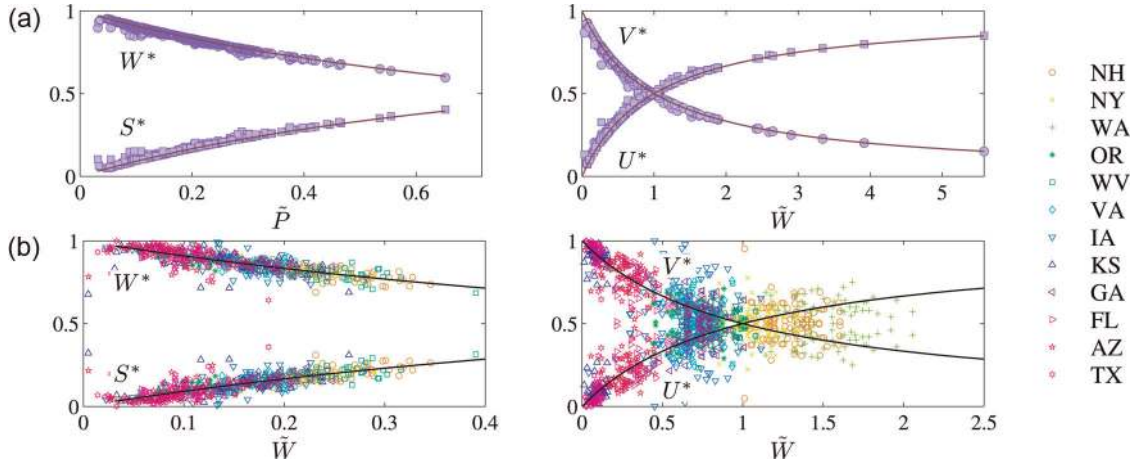

Figure 7. Nondimensional annual estimates of (left) W^* and S^* and (right) U^* and V^* versus annual climatic drivers $\tilde{P}$ and $\tilde{W}$ for all MOPEX catchments: (a) between-catchment variability of mean annual water balance and (b) interannual variability in 12 selected MOPEX catchments (see Figure 5 and Table 1). Points represent data (equations (10) and (11)), and the solid lines are theoretical lines (equations (15) and (16)).

[55] Vaporization fraction

$$K_V = \frac{V^*}{\left(1 + \frac{K}{\tilde{P}}\right)} \left(\frac{K}{\tilde{P}} + W^*\right), \tag{22}$$

[56] Runoff fraction

$$K_R = \frac{1}{\left(1 + \frac{K}{\tilde{P}}\right)} \left[S^* + U^*\left(\frac{K}{\tilde{P}} + W^*\right)\right]. \tag{23}$$

[57] We can reformulate these expressions in terms of the driving variables $\tilde{P}$ and $\tilde{V}$. The resulting expressions, after combining with equations (13)–(16), are as follows (the details of the derivation are not presented here for sake of brevity):

[58] Horton index

$$K_H = \frac{(1 + \tilde{P})\,\tilde{V}}{K + \tilde{P} + K\tilde{P} + \tilde{V} + \tilde{V}\tilde{P}}, \tag{24}$$

[59] Base flow fraction

$$K_B = \frac{(K + \tilde{P} + K\tilde{P})^2}{(K + \tilde{P})\,(1 + \tilde{P})\,(K + \tilde{P} + K\tilde{P} + \tilde{V} + \tilde{V}\tilde{P})}, \tag{25}$$

[60] Vaporization fraction

$$K_V = \frac{(K + \tilde{P} + K\tilde{P})\,\tilde{V}}{(K + \tilde{P})\,(K + \tilde{P} + K\tilde{P} + \tilde{V} + \tilde{V}\tilde{P})}, \tag{26}$$

[61] Runoff fraction

$$K_R = \frac{K^2(1 + \tilde{P}) + K\tilde{P}(2 + \tilde{P}) + \tilde{P}^2(1 + \tilde{V})}{(K + \tilde{P})\,(K + \tilde{P} + K\tilde{P} + \tilde{V} + \tilde{V}\tilde{P})}. \tag{27}$$

[62] Let us take the example of the Horton index K_H. As can be seen in equation (24), K_H is a function of the two driving variables, $\tilde{P}$ and $\tilde{V}$, and the coefficient K. Estimates of the parameter K for most of the 377 catchments ranged from -0.04 to 0.04. These relatively small values justify the assumption that $K = 0$, in which case expressions (24)–(27) become considerably simplified without loss of accuracy, as shown in equations (28)–(31). For the case $K = 0$ and defining a new aridity index $\varphi = \tilde{V}/\tilde{P}$, the resulting simpler expressions for K_H, K_B, K_V, and K_R are

[63] Horton index

$$K_H = \frac{(1 + \tilde{P})\,\tilde{V}}{\tilde{P} + \tilde{V} + \tilde{V}\tilde{P}} = \frac{(1 + \tilde{P})\,\varphi}{1 + \varphi + \tilde{P}\varphi}, \tag{28}$$

[64] Base flow fraction

$$K_B = \frac{\tilde{P}}{(1 + \tilde{P})\,(\tilde{P} + \tilde{V} + \tilde{V}\tilde{P})} = \frac{1}{(1 + \tilde{P})\,(1 + \varphi + \tilde{P}\varphi)}, \tag{29}$$

[65] Vaporization fraction

$$K_V = \frac{\tilde{V}}{(\tilde{P} + \tilde{V} + \tilde{V}\tilde{P})} = \frac{\varphi}{1 + \varphi + \tilde{P}\varphi}, \tag{30}$$

[66] Runoff fraction

$$K_R = \frac{\tilde{P}(1 + \tilde{V})}{(\tilde{P} + \tilde{V} + \tilde{V}\tilde{P})} = \frac{1 + \tilde{P}\varphi}{1 + \varphi + \tilde{P}\varphi}. \tag{31}$$

[67] The effect of making the assumption of $K = 0$ on the resulting estimates of the four indices was evaluated for the 377 catchments and was found to be insignificant (RMSE for the four indices ranged between 2% and 5%).

[68] These expressions suggest that annual water balance is governed by two dimensionless similarity variables: a new aridity index $\varphi = \tilde{V}/\tilde{P}$ and a scaled annual precipitation $\tilde{P}$. The aridity index φ can be seen as a ratio of vaporization potential to precipitation, and in this sense it is equivalent to the classical aridity index E_p/P of *Budyko* [1974]. We have tried to determine if an association can be found between $\varphi = \tilde{V}/\tilde{P}$ and E_p/P by regressing them against each other using data from the 377 catchments and found a weak relationship of the type $\varphi = 4.0\,E_p/P - 1.875$ with $R^2 = 0.461$. On the other hand, $\tilde{P}$ is a ratio of precipitation to the wetting potential (the latter being equivalent to storage capacity of the soil). Given this equivalence, one can see the similarity of the resulting expressions to functional forms adopted to describe the Budyko curve [*Milly*, 1994a, 1994b; *Zhang et al.*, 2001; *Yang et al.*, 2007], which were derived through other means. In two companion papers, Zanardo et al. (submitted manuscript, 2011) have derived almost identical expressions for the Horton index based on a process model, and Voepel et al. (submitted manuscript, 2011) have derived regression relationships for the Horton index in terms of the aridity index and the catchment average slope and elevation. The result for the base flow fraction is interesting, and to our knowledge, no equivalent result has appeared in the literature. It should be noted that the collapsed forms of the Ponce and Shetty model and partitioning expressed in equations (28)–(31) cannot themselves be used for prediction in the normal sense since the driving variables $\tilde{P}$ and φ are themselves partially derived from the fitted functional parameters. Rather, by introducing these expressions, we hope to reveal the underlying functional forms that seem to unify the variations in responses between catchments and between years.

[69] In sections 5.2 and 5.3, we will evaluate the ability of these simplified expressions to reproduce estimates of these indices (Horton index, base flow fraction, vaporization fraction, and the runoff fraction) from observed data for the MOPEX catchments.

5.2. Between-Catchment Variability of Mean Annual Water Balance: Regional Patterns

[70] The theoretical formulations presented in section 5.1 indicate that for the case where $K = 0$ is reasonable, all four water balance metrics, i.e., K_H, K_B, K_V, and K_R, are functions of just two nondimensional similarity variables, namely, $\varphi = \tilde{V}/\tilde{P}$ and $\tilde{P}$. This idea is tested by estimating the four

indices from data directly from the MOPEX catchments and comparing them against theoretical estimates obtained by applying equations (28)–(31). This is done both for mean annual water balances and for interannual variability of water balances. The results for mean annual water balances are presented in Figure 8, in which estimates of K_H, K_B, K_V, and K_R are expressed as a function of the aridity index $\varphi = \tilde{V}/\tilde{P}$. The empirical results are presented in the form of data points, whereas the theoretical estimates are presented as lines for three different values of $\tilde{P}$.

[71] A number of features can be highlighted with respect to the results presented in Figure 8. First, in all cases, there is remarkable tightness in the relationship between the four indices and the aridity index $\varphi = \tilde{V}/\tilde{P}$, which is clearly seen as the primary determinant of mean annual water balance, with $\tilde{P}$ playing only a secondary role. In the case of K_V and K_R, the scatter in the relationship, which is caused by $\tilde{P}$, increases with increasing aridity. On the other hand, in the case of the Horton index K_H and to an extent the base flow fraction K_B the scatter is less for the entire range of aridity values and, in fact, decreases with increasing aridity. The theoretical curves confirm these empirical observations: the width between the $\tilde{P}$ contours widens with increasing $\varphi = \tilde{V}/\tilde{P}$ for K_V and K_R, whereas it shrinks with increasing $\varphi = \tilde{V}/\tilde{P}$ for K_H and K_B. The remarkable tightness in the relationship between K_H (and to an extent also K_B) and $\varphi = \tilde{V}/\tilde{P}$, compared to the other two indices, supports the observations and explanations of *Horton* [1933], which were reiterated by *Troch et al.* [2009].

[72] The form of the functional relationship between K_V and $\varphi = \tilde{V}/\tilde{P}$ is similar to the shape of its equivalent, the Budyko curve, which is mirrored in its complementary runoff fraction K_R, which is not surprising since $K_R = 1 - K_V$. Finally, the results obtained for K_B, on the other hand, are quite interesting, indicating that the fraction of precipitation partitioned to slow flow is highest in wet catchments (as high as 0.7) and decreases with increasing aridity. This phenomenon might be due to the coevolution of the vegetation with the soils and topographic features that govern subsurface flow as part of the self-organization of the vegetation with the climate, as proposed by *Horton* [1933]. This is partially confirmed by the results of Zanardo et al. (submitted manuscript, 2011) regarding soil properties and by the results of Voepel et al. (submitted manuscript, 2011), whose results demonstrated links between the Horton index and both the topography and estimates of vegetation cover (e.g., annual maximum NDVI).

[73] We also investigated spatial patterns in these relationships to see if we can discover any regional patterns in the water balance behavior. Figure 9 presents spatial patterns of the estimates (from raw data) of K_H, K_V, K_B, and K_R. To interpret these patterns of mean annual water balance behavior, we also present, in Figure 10, the spatial patterns of the two similarity parameters $\varphi = \tilde{V}/\tilde{P}$ and $\tilde{P}$ for the 377 MOPEX catchments. The results show a clear, strong correspondence between the water balance indices and the aridity index $\varphi = \tilde{V}/\tilde{P}$. Regions of high values of φ (e.g., Midwest, South, and Southwest) exhibit relatively high values of K_H and K_V and low values of K_B and K_R (as expected from the functional forms presented in equations (28)–(31)), with opposite behavior in regions with low values of φ (e.g., Appalachia). The reason for the high values of aridity index in the Midwest could be due to a combination of factors: low to moderate precipitation $\tilde{P}$, moderate to high atmospheric demand, and deep soils, which are reflected in high $\tilde{V}$. One can also see in Figure 11 that the highest values of the base flow fraction K_B are seen in the mountainous Appalachian region in the eastern United States and mountainous catchments in the West. The role of topography is clearly evident.

5.3. Trends in Between-Year Variability of Water Balance: Space-Time Symmetry

[74] We have now established that the relationships in equations (28)–(31), along with the nondimensional similarity parameters, are able to quantify the mean annual water balance for a large number of catchments over a range of ecoregions across the United States. How well can the same relationships also reproduce the interannual variability in individual catchments? This goes to the heart of the question of the symmetry between between-catchment

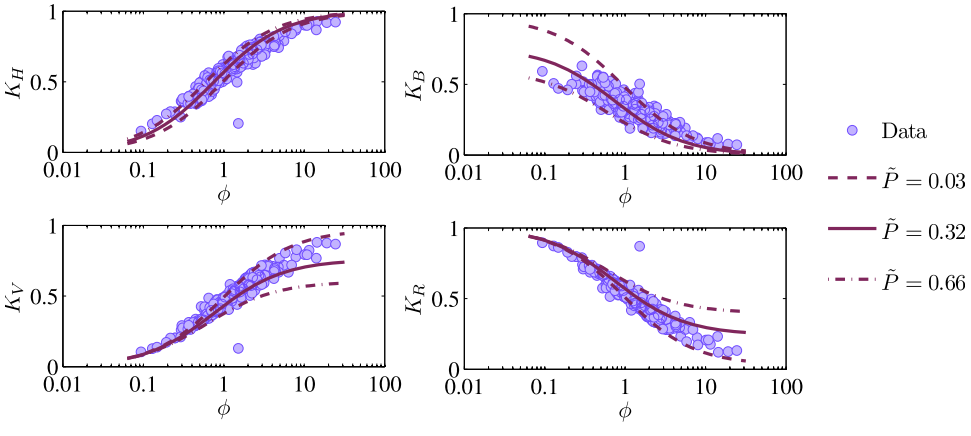

Figure 8. Estimates of nondimensional Horton index K_H, vaporization fraction K_V, base flow fraction K_B, and runoff fraction K_R for mean annual water balance based on raw data for 377 MOPEX catchments (points). (Equation (19) is used to estimate data points, and equations (28)–(30) are used to plot the lines for different values of $\tilde{P}$.)

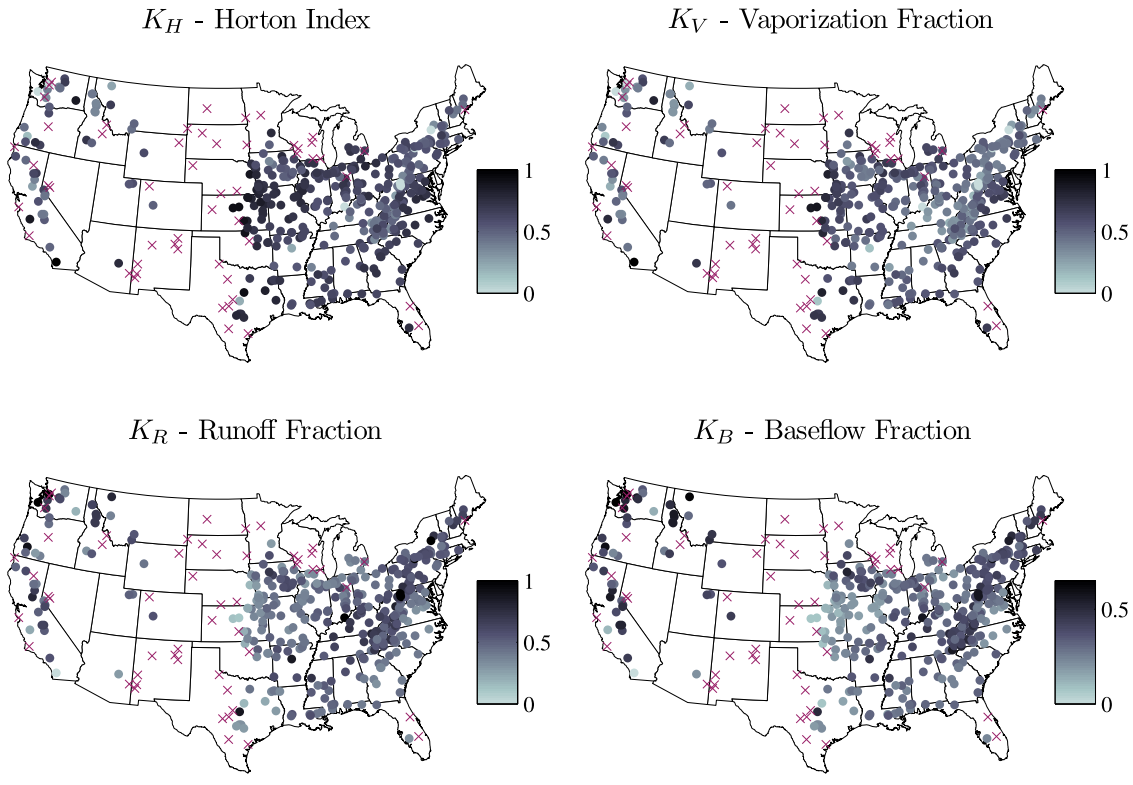

Figure 9. Spatial variations in the 50 year mean annual value of the Horton index K_H, vaporization fraction K_V, base flow fraction K_B, and runoff fraction K_R as defined by equation (19) and estimated from empirical data.

and between-year variability of annual water balances. Answering this question and understanding the underlying climate-landscape controls will have to be the first steps toward predictions of the responses of catchments undergoing change, especially climate change, through supporting the application of "space for time" substitutions.

[75] Figure 11 (left) presents the results for the three indices (K_H, K_V, and K_B) as a function of annual $\tilde{P}$ (variable between years) with $\tilde{V}$ as a fixed parameter for each site, with humid sites having lower values of $\tilde{V}$ and more arid sites having higher values. The data points in different symbols are based on actual water balance estimates for the 12 catchments (ranging from dark grey points, which are arid catchments, to light grey points, which are humid catchments), and the lines (using the same colors) are calculated using the theoretical model (equations (28)–(31)) and so are trajectories of constant $\tilde{V}$. A number of features can be highlighted here. First, the nondimensional models for the indices capture very well the interannual variability of the indices for all 12 catchments. We also find that estimates of K_H and K_V decrease with increasing $\tilde{P}$ between years but increase with increasing values of $\tilde{V}$ (i.e., going from humid to arid), which is partly a measure of aridity. On the other hand, the results for K_B are exactly opposite to those of K_H and K_V, in respect to both $\tilde{P}$ and $\tilde{V}$. Another interesting result is that the slope of the relationship of K_H with $\tilde{P}$ is smaller

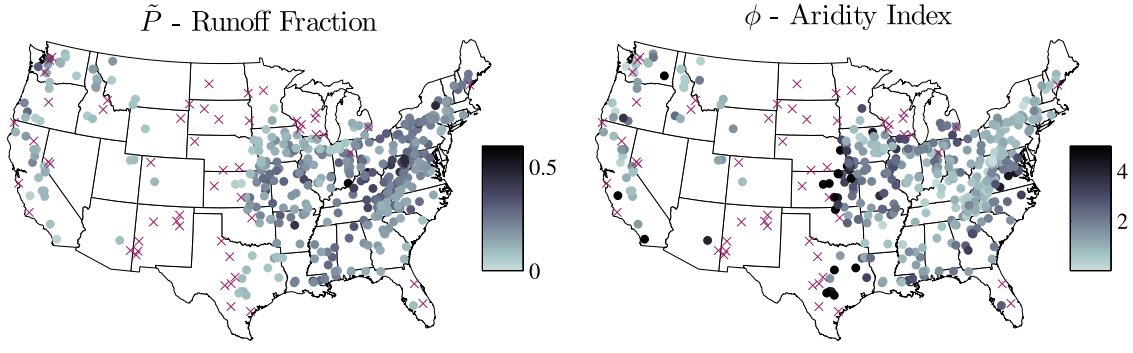

Figure 10. Spatial variations of mean annual values of the aridity index $\varphi = \tilde{V}/\tilde{P}$ (see equation (12) for definition of $\tilde{P}$and $\tilde{V}$) and mean annual rescaled precipitation $\tilde{P}$ estimated from climate data and the *Ponce and Shetty* [1995a, 1995b] parameters.

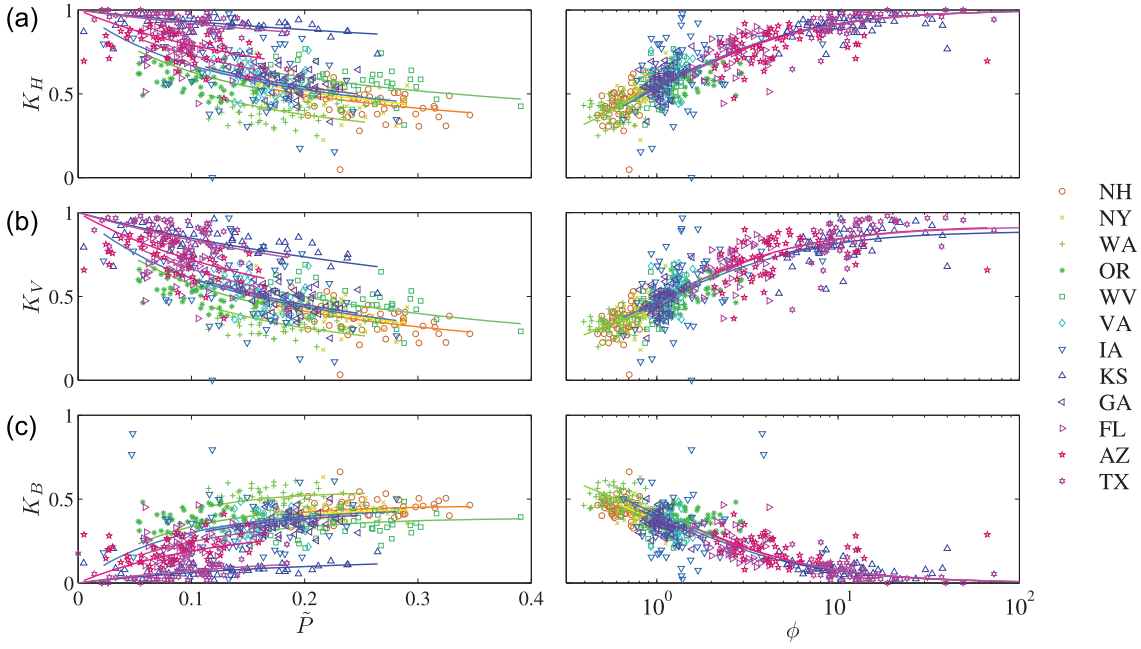

Figure 11. Estimates of nondimensional (a) Horton index K_H, (b) vaporization fraction K_V, and (c) base flow fraction K_B based on actual data (data points, equation (19)) and predictions by the nondimensional model as trajectories of constant $\tilde{V}$ (equations (28), (29), and (30), respectively) for 12 selected catchments (left) as functions of $\tilde{P}$ and $\tilde{V}$ and (right) as functions of $\varphi = \tilde{V}/\tilde{P}$.

than the corresponding slope for K_V, true for all catchments, suggesting that there is considerably more damping of the precipitation variability as it manifests in the Horton index as compared to the Budyko curve. In other words, in relative terms, the Horton index remains relatively more constant between years. This result is at the heart of *Horton*'s [1933] hypothesis and prompts a detailed analysis of the damping that occurs as precipitation is partitioned into its various components, which is presented in detail in section 6.

[76] Another way to show the same results, as a way to draw an analogy with the results for mean annual water balances presented in Figure 8, is to plot the indices K_H, K_V, K_B, and K_R as functions of estimates of a variable aridity index $\varphi = \tilde{V}/\tilde{P}$ estimated for each year on the basis of the 50 year precipitation record. In this case, the results are presented in Figure 11 (right), using the same color coding as before. Once again, the data points are based on actual water balance estimates, and the lines are calculated from the theoretical model (equations (28)–(31)) and so are trajectories of constant $\tilde{V}$. Two major features can be highlighted in these results. First, in all three cases, but especially in the case of K_B, the results show a large reduction of scatter and show coherent relationships that are identical to the between-catchment relations for the 377 catchments presented in Figure 8. Second, in the case of K_H and K_B, even the theoretical curves almost collapse into a single curve. This is not so in the case of K_V, with the theoretical lines diverging for the two most arid catchments. This is consistent with results presented in Figure 8 for K_V and K_R, in which lines for different mean annual $\tilde{P}$ values diverge with increasing φ. In each case, however, the color coding allows us to see the parallels between the between-year variability shown here with the between-catchment variability presented in Figure 8. Taken together with the patterns displayed in Figure 8, these results indicate a remarkable symmetry between spatial (between-catchment) variability of mean annual water balances and the general trends in the temporal (between-year) variability of annual water balances, which has important implications for predictions of hydrologic change.

[77] While these results showed that the nondimensional model is indeed able to reproduce the general trends of between-year variability, the scatter in the results indicates that the responses in individual years are not well predicted. The scatter in the interannual variability could be a result of other factors, including the effects of within-year and within-catchment variability of climatic inputs and their interactions with landscape properties. Clearly, a theory that is only based on analysis of annual rainfall-runoff data, such as that of L'vovich, cannot be expected to reproduce these effects. For this we need models that explicitly incorporate intra-annual and intracatchment variabilities [*Jothityangkoon and Sivapalan*, 2009; *Potter and Zhang*, 2009]. This is left for future research.

6. Damping of Precipitation Variability Within the Catchment System

[78] The results presented in sections 5.2 and 5.3 above have demonstrated that the Ponce and Shetty model can also capture the general trends in the between-year variability in the partitioning of annual precipitation. Using this framework, we can analyze the hypothesis first put out by *Horton* [1933] and recently taken up again by *Troch et al.* [2009] that interannual variability in the Horton index is damped compared to the variability in the driving precipitation. These results were motivated by the results presented

in Figures 11a and 11b, including the observation that interannual variability of K_H was more damped than that of K_V, with the slope of the fitted trends in both cases decreasing with increasing $\tilde{V}$, a relative measure of aridity. This shows that the interannual variability in the vaporization as a fraction of wetting is smaller than the same vaporization as a fraction of the total precipitation.

[79] We can use the Ponce and Shetty model to quantify the damping of interannual variability in precipitation as it propagates through the catchment system. This allows us to map the degree of damping involved and to reveal related spatial patterns and relate the damping of this variability to the functional properties of the catchment. A first-order approximation for the variance of the Horton index can be derived in terms of the mean and standard deviation of annual precipitation (μ_P and σ_P) and the four Ponce-Shetty parameters, W_p, V_p, λ_s and λ_u, by taking a first-order Taylor series expansion of the definition of the variance around the expected value μ_P.

$$\sigma^2_{H\text{pred}} = E\left[\{f_H(P) - \mu_H\}^2\right] \approx \{f_H(\mu_P)\}^2\sigma^2_P, \tag{32}$$

where f_H is the Ponce and Shetty model for the Horton index V/W, where W and V are given by equations (5) and (6), respectively. Using the functional forms presented in equations (5) and (6), we can express the transformation of the variability of annual precipitation into variability in the Horton index in terms of a damping factor D_H:

$$\sigma_H = D_H \frac{\sigma_P}{\mu_P}. \tag{33}$$

[80] Similar expressions can be written for the vaporization fraction V/P in terms of damping factor D_V. These expressions are

$$D_H = \mu_P \frac{VW' - V'W}{W^2}, \tag{34}$$

$$D_V = \frac{V}{\mu_P} - V', \tag{35}$$

where V and W are the Ponce and Shetty functions expressed in terms of P and V' and W' are the derivatives of these functions with respect to P. These two damping coefficients represent the degree to which the variability in P is reduced by the partitioning functions of the catchment. Furthermore, their ratio D_H/D_V is a measure of the reduction in the variability of the Horton index relative to the overall water balance. Small values indicate that even when the variability in the fraction of annual precipitation converted to vaporization is large, the variability in vaporization as a fraction of wetting is small.

[81] To compare these estimates to data, we must account for the contribution of the residual error in the model estimates of the Horton Index and vaporization fraction to the observed data. In precise terms, the annual observed Horton indices can be represented as the sum of the model estimates and the error $H_{\text{obs}} = H_{\text{pred}} + \varepsilon_H$. The observed variance is therefore the sum of the predicted variance and the error variance $\sigma^2_{H\text{obs}} = \sigma^2_{H\text{pred}} + \sigma^2_{\varepsilon_H}$. Using this relationship (and a similar one for the vaporization), we can estimate the damping factors from data, corrected for the model error.

$$D_H \approx \frac{\sqrt{S^2_{H\text{obs}} - S^2_{\varepsilon H}}}{S_P/\bar{P}}, \tag{36}$$

$$D_V \approx \frac{\sqrt{S^2_{V\text{obs}} - S^2_{\varepsilon V}}}{S_P/\bar{P}}, \tag{37}$$

where $S^2_{X\text{obs}}$ and $S^2_{\varepsilon X}$ are the sample estimates of the variance and residual error of the Horton index and the vaporization fraction.

[82] Figure 12 shows the range of values of the damping coefficients and the damping ratio and the ability of the Ponce and Shetty model to predict them, which is generally good once the error variance is accounted for. Both coefficients tend to be smaller than 1, indicating that there is significant damping of the precipitation variability in the Horton Index and vaporization fraction. However, the damping coefficient of the Horton index is generally smaller. Indeed, the damping ratio is generally less than 1. This result supports the idea that the functional properties

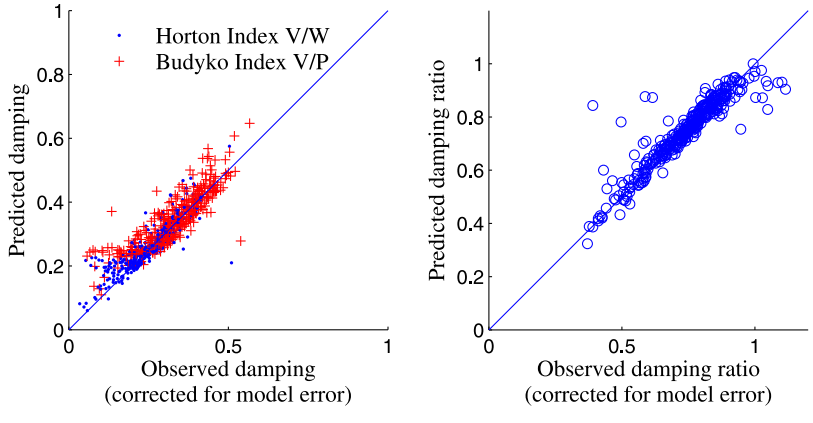

Figure 12. Observed and predicted damping coefficients D_H and D_V and the damping ratio D_H/D_V.

of catchments lead to a suppression of the variability in the Horton index.

[83] The nondimensionalization described in equations (28)–(31) can provide insight into the functional behavior underlying this damping. If instead of the Horton Index and vaporization fraction, we consider the modified nondimensional indices described in section 5, we can derive an expression for the damping coefficients and ratio. For the case where $K = 0$ these are

$$D_{KH} = \frac{\tilde{P}\tilde{V}}{(\tilde{P}\tilde{V} + \tilde{P} + \tilde{V})^2}, \tag{38}$$

$$D_{KV} = \frac{\tilde{P}\tilde{V}(1 + \tilde{V})}{(\tilde{P}\tilde{V} + \tilde{P} + \tilde{V})^2}. \tag{39}$$

[84] And the damping ratio becomes simply

$$\frac{D_{KH}}{D_{KV}} = \frac{1}{(1 + \tilde{V})}. \tag{40}$$

[85] This suggests that the degree to which the Horton index is damped relative to the vaporization fraction V/P is a function only of $\tilde{V}$. When $\tilde{V}$ is close to zero, the additional damping is minimal. When it is large, the interannual variability in Horton index V/W is much smaller than that of the vaporization fraction V/P. This confirms the qualitative observations from Figures 11a (left) and 11b (left).

[86] Figure 13 shows the spatial pattern of the damping ratio as defined in equation (40). This map shows that the damping of interannual variation in the Horton index (relative to the vaporization fraction) is strongest in the middle of the continental United States and along the East Coast. In Appalachia and in the West the damping ratio is less. To interpret this pattern, it is necessary to recall that $\tilde{V}$, and therefore the damping ratio, is controlled by all four functional parameters. Large values of $\tilde{V}$ are associated with large vaporization potentials, small wetting potentials, small thresholds for slow flow, and large thresholds for quick flow. Examination of the spatial patterns in these variables shown in Figure 6 suggests that the spatial pattern of the damping ratio is not dominated by the spatial pattern in any one of these but, rather, by their combined spatial variations.

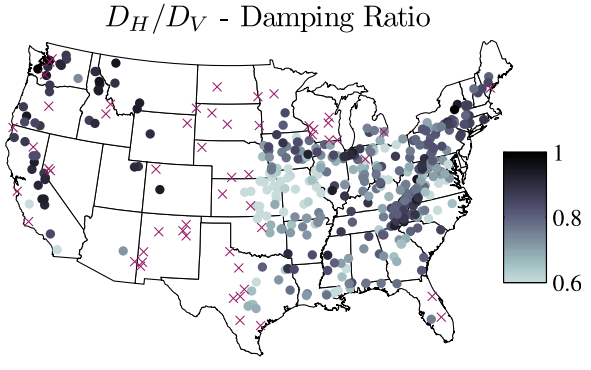

Figure 13. Spatial distribution of the damping ratio D_H/D_V for the 377 MOPEX catchments.

7. Discussion and Conclusions

[87] In this paper we have reintroduced the functional approach, pioneered by *L'vovich* [1979] and extended by *Ponce and Shetty* [1995a, 1995b], to the analysis of water balance variability at the annual time scale, including both between-catchment (i.e., regional) and between-year (i.e., interannual) variability. An important feature of the L'vovich–Ponce-Shetty functional theory is that in addition to predicting total annual evaporation and runoff, it is able to make predictions of the spatial (between-catchment) and temporal (between-year) variability of both runoff components (quick flow and slow flow) as well as vaporization. In this sense the theory is a significant advance over other currently available empirical theories [e.g., *Budyko*, 1974; *Zhang et al.*, 2001], which can only predict total runoff. This feature of the theory gives it an additional advantage toward making predictions of changes in annual water balance due to the effects of global change (climate, land use, or land cover change).

[88] In the L'vovich approach, precipitation is first partitioned into wetting and quick flow, and in the second stage, the wetting is further partitioned into evaporation and slow flow. On the basis of the published empirical results presented by L'vovich for a large number of catchments around the world, *Ponce and Shetty* [1995a, 1995b] derived common functional forms for each stage of the partitioning that can be extracted from observed rainfall-runoff data. In this study we have implemented the L'vovich–Ponce-Shetty theory to well over 300 MOPEX catchments across the continental United States and characterized the heterogeneity of mean annual water balances. The results of the analysis showed interesting regional patterns of the four parameters associated with the *Ponce and Shetty* [1995a, 1995b] theory, although they have yet to be explained in terms of regional patterns of climatic and/or landscape properties.

[89] On the other hand, conversion of the Ponce and Shetty functional forms into nondimensional forms helped to extract an invariant and parameter-free relationship that underlies the observed heterogeneity of site-specific relationships seen in the study catchments and is therefore transferable regionally. This universal relationship can easily be expressed in the form of a competition between alternative catchment functions applicable at the surface and subsurface levels. Key nondimensional similarity parameters are identified that serve to connect the regional or universal behavior to site-specific response characteristics. This study also looked at interannual variability of annual water balance partitioning in 12 representative catchments selected in different ecoregions. When this is expressed in the same nondimensional forms as before, the universal competitive relationship continued to hold even in the case of interannual variability.

[90] The study also explored the ability of the nondimensional L'vovich–Ponce-Shetty formulation to reproduce metrics of both spatial (between-catchment) variability of mean annual water balance and temporal (between-year) variability of annual water balance. Four metrics were

assessed: the Horton index (ratio of vaporization to wetting [*Troch et al.*, 2009]), a vaporization fraction (ratio of vaporization to precipitation, the same as the Budyko curve), a base flow fraction (ratio of slow flow to precipitation), and a runoff fraction (the same as the annual runoff coefficient, ratio of total runoff to precipitation). Using the nondimensional formulation, we were able to derive analytical expressions for all four indices in terms of two nondimensional variables: a new aridity index and a scaled precipitation (ratio of annual precipitation to wetting potential). Estimates of these metrics based on the derived functional forms were tested against estimates based on data, and it was demonstrated that the normalized observations collapsed onto the expected curve.

[91] Interestingly, the same functional forms were also shown to be able to predict the general trends of interannual variability in 12 catchments selected from different ecoregions. This once again highlighted a remarkable symmetry between spatial (between-catchment) variability and general trends of temporal (between-year) variability. Interannual variability that arises from within-year and within-catchment variability of climate inputs cannot be captured by the L'vovich theory, and in many cases this variability is significant. This paper investigated the propagation of interannual precipitation variability through the catchment system and developed measures of the relative damping exhibited in various metrics of annual water balance, notably the Horton index and the vaporization fraction. It was found that the damping of the Horton index between years was more than that of the vaporization fraction. The damping ratio is larger in more arid catchments than in more humid catchments, confirming *Horton*'s [1933, p. 456] hypothesis that "natural vegetation of a region tends to develop to such an extent that it can utilize the largest possible proportion of the available soil moisture supplied by infiltration," as also emphasized by *Troch et al.* [2009].

[92] There is considerable interest in predicting the effects of long-term climate variability and climate change on water balances. One of the approaches to predicting the effects of temporal change in climate is the method of "space for time substitution," i.e., using observations across a climate gradient in space to predict the effects of a future climate change in the time domain. The results presented in this paper give us confidence that the spatial patterns of mean annual water balance presented in this study, and the dominant process controls that were identified, can be used to predict changes in water balance due to future climatic changes. The companion paper by *Harman et al.* [2011] presents the results of a sensitivity study that assesses the relative contributions of precipitation to the annual water balance changes, including measures of the resilience of the catchment system to these changes.

[93] The empirical relationships derived in this paper, within the *L'vovich* [1979] and *Ponce and Shetty* [1995a, 1995b] framework and based on annual rainfall-runoff data from the 377 MOPEX catchments, can be seen as emergent properties. Nevertheless, application of these analytical expressions for predictions in ungauged basins requires that the associated parameters can be estimated a priori. This will not be feasible until a way can be found to link the associated effective (i.e., emergent) parameters to standard data sets of climatic and landscape properties. To this end, it is important to carry out detailed process-based modeling studies to explore how Ponce and Shetty–type functional forms emerge through small-scale (time and space) processes and process interactions and associated scale effects. In cold regions this analysis must also include explicit treatment of snow (snowfall and snowmelt). In a parallel study, Zanardo et al. (submitted manuscript, 2011) have used a simple stochastic water balance model to explore climate-landscape controls on the Horton index and developed functional representations that are almost identical to those obtained in this study. Further work combining these two modeling approaches can lead to productive avenues for estimating the Ponce and Shetty parameters in ungauged catchments. The possible connection between the analytical Ponce and Shetty–type functional forms (and associated parameter values) and detailed process descriptions and measurable physical catchment/climate characteristics is left for further study. Thompson et al. (submitted manuscript, 2010) present a theoretical framework within which such an exploration can be carried out, including the relationship between spatial patterns of vegetation and water balance within a catchment.

[94] This paper represents an example of comparative hydrology, where insights into the hydrological responses are obtained by comparing and contrasting a diversity of catchments in different climatic or ecoregions rather than detailed process explorations in a single catchment [*Falkenmark and Chapman*, 1989; *Sivapalan*, 2009]. In this case we looked at rainfall-runoff responses only. However, given the presence of space-time symmetry in annual water balance variability and the key role played by vegetation in bringing this about [*Horton*, 1933; *Troch et al.*, 2009], one can be tempted to ask the question whether a similar space-time symmetry can be seen in vegetation cover and its functioning resulting from adaptations to changing climate in time and space. This is a critical ecohydrological question that needs to be answered on the basis of both rainfall-runoff data and data on spatial patterns of vegetation cover, which are routinely available these days through remote sensing. The paper by Voepel et al. (submitted manuscript, 2011) as well as a paper by P. D. Brooks et al. (Quantifying regional-scale ecosystem response to changes in precipitation: Not all rain is created equal, submitted to *Water Resources Research*, 2010) will present results connecting annual water balance to measures of vegetation cover, including interannual variability, opening up exciting avenues for interdisciplinary research.

[95] **Acknowledgments.** Work on this paper commenced during the Summer Institute organized at the University of British Columbia (UBC) during June–July 2009 as part of the NSF-funded project "Water Cycle Dynamic in a Changing Environment: Advancing Hydrologic Science through Synthesis" (NSF grant EAR-0636043, M. Sivapalan, PI). We acknowledge the support and advice of numerous participants at the Summer Institute (students and faculty mentors). Work on the paper was also partially supported by the NSF project "Understanding the Hydrologic Implications of Landscape Structure and Climate—Toward a Unifying Framework of Watershed Similarity" (grant EAR-0635998, T. Wagener, PI). Special thanks are owed to Mateij Durcik for help with the background data preparation and analysis of the MOPEX catchments. Thanks are also owed to Marwan Hassan and the Department of Geography of UBC for hosting the Summer Institute and for providing outstanding facilities, without which this work would not have been possible.

References

Arnold, J. G., and P. M. Allen (1999), Automated methods for estimating baseflow and ground water recharge from streamflow records, *J. Am. Water Resour. Assoc.*, *35*(2), 411–424.

Black, P. E. (1997), Watershed functions, *J. Am. Water Resour. Assoc.*, *33*(10), 1–11.

Botter, G., A. Porporato, I. Rodriguez-Iturbe, and A. Rinaldo (2007), Basin-scale soil moisture dynamics and the probabilistic characterization of carrier hydrologic flows: Slow, leaching-prone components of the hydrologic response, *Water Resour. Res.*, *43*, W02417, doi:10.1029/2006WR005043.

Budyko, M. I. (1974), *Climate and Life*, Elsevier, New York.

Dooge, J. C. I. (1992), Sensitivity of runoff to climate change: A Hortonian approach, *Bull. Am. Meteorol. Soc.*, *73*(12), 2013–2024.

Duan, Q., et al. (2006), Model Parameter Estimation Experiment (MOPEX): An overview of science strategy and major results from the second and third workshops, *J. Hydrol.*, *320*(1-2), 3–17.

Eagleson, P. S. (1978), Climate, soil, and vegetation, a simplified model of soil moisture movement in liquid phase, *Water Resour. Res.*, *14*(5), 722–730.

Eagleson, P. S., and R. R. Tellers (1982), Ecological optimality in water-limited natural soil-vegetation systems. 2. Tests and applications, *Water Resour. Res.*, *18*(2), 341–354.

Eckhardt, K. (2005), How to construct recursive digital filters for baseflow separation, *Hydrol. Processes*, *19*, 507–515.

Falkenmark, M., and T. Chapman (1989), *Comparative Hydrology—An Ecological Approach to Land and Water Resources*, 479 pp., U. N. Educ., Sci., and Cultural Organ., Paris.

Farnsworth, R. K., E. S. Thompson, and E. L. Peck (1982), Evaporation atlas for the contiguous 48 United States, *NOAA Tech. Rep. NWS 33*, 26 pp., NOAA, Silver Spring, Md.

Harman, C. J., P. A. Troch, and M. Sivapalan (2011), Functional model of water balance variability at the catchment scale: 2. Elasticity of fast and slow runoff components to precipitation change in the continental United States, *Water Resour. Res.*, W02523, doi:10.1029/2010WR009656.

Horton, R. E. (1933), The role of infiltration in the hydrologic cycle, *Eos Trans. AGU*, *14*, 446–460.

Jothityangkoon, C., and M. Sivapalan (2009), Framework for exploration of climatic and landscape controls on catchment water balance, with emphasis on inter-annual variability, *J. Hydrol.*, *371*, 154–168, doi:10.1016/j.jhydrol.2009.03.030.

L'vovich, M. I. (1979), *World Water Resources and Their Future*, translated from Russian by R. L. Nace, 415 pp., AGU, Washington, D. C.

Lyne, V., and M. Hollick (1979), Stochastic time-variable rainfall-runoff modelling, in *Proceedings, Institute of Engineers Australia National Conference*, Inst. Engrs., Canberra, Australia, ACT. Publ. 79/10: 89–93.

Milly, P. C. (1994a), Climate, soil water storage, and the average annual water balance, *Water Resour. Res.*, *30*(7), 2143–2156.

Milly, P. C. (1994b), Climate, interseasonal storage of soil water and the annual water balance, *A dv. Water Resour.*, *17*, 19–24.

Peel, M. C., T. A. McMahon, and B. L. Finlayson (2010), Vegetation impact on mean annual evapotranspiration at a global catchment scale, *Water Resour. Res.*, *46*, W09508, doi:10.1029/2009WR008233.

Ponce, V. M., and A. V. Shetty (1995a), A conceptual model of catchment water balance. 1. Formulation and calibration, *J. Hydrol.*, *173*, 27–40.

Ponce, V. M., and A. V. Shetty (1995b), A conceptual model of catchment water balance. 2. Application to runoff and baseflow modeling, *J. Hydrol.*, *173*, 41–50.

Porporato, A., E. Daly, and I. Rodriguez-Iturbe (2004), Soil water balance and ecosystem response to climate change, *Am. Nat.*, *164*, 625–632.

Potter, N. J., and L. Zhang (2009), Interannual variability of catchment water balance in Australia, *J. Hydrol.*, *369*, 120–129.

Potter, N. J., L. Zhang, P. C. D. Milly, T. A. McMahon, and A. J. Jakeman (2005), Effects of rainfall seasonality and soil moisture capacity on mean annual water balance for Australian catchments, *Water Resour. Res.*, *41*, W06007, doi:10.1029/2004WR003697.

Reggiani, P., M. Sivapalan, and S. M. Hassanizadeh (2000), Conservation equations governing hillslope responses: Exploring the physical basis of water balance, *Water Resour. Res.*, *36*(7), 1845–1864.

Salvucci, G. D., and D. Entekhabi (1995), Hillslope and climatic controls on hydrologic fluxes, *Water Resour. Res.*, *31*(7), 1725–1739, doi:10.1029/95WR00057.

Sivapalan, M. (2009), The secret to "doing better hydrological science": Change the question!, *Hydrol. Processes*, *23*, 1391–1396, doi:10.1002/hyp.7242.

Soil Conservation Service (1985), *National Engineering Handbook, Section 4, Hydrology*, U.S. Dep. of Agric., Washington, D. C.

Troch, P. A., G. F. Martinez, V. R. N. Pauwels, M. Durcik, M. Sivapalan, C. J. Harman, P. D. Brooks, H. V. Gupta, and T. E. Huxman (2009), Climate and vegetation water-use efficiency at catchment scales, *Hydrol. Processes*, *23*, 2409–2414, doi:10.1002/hyp.7358.

Wagener, T., M. Sivapalan, P. A. Troch, and R. A. Woods (2007), Catchment classification and hydrologic similarity, *Geogr. Compass*, *1*(4), 901–931, doi:10.1111/j.1749-8198.2007.00039.x.

Wagener, T., M. Sivapalan, and B. McGlynn (2008), Catchment classification and services—Toward a new paradigm for catchment hydrology driven by societal needs, in *Encyclopedia of Hydrological Sciences*, edited by M. G. Anderson, John Wiley, Chichester, U. K.

Wang, T., E. Istanbulluoglu, J. Lenters, and D. Scott (2009), On the role of groundwater and soil texture in the regional water balance: An investigation of the Nebraska Sand Hills, USA, *Water Resour. Res.*, *45*, W10413, doi:10.1029/2009WR007733.

Yang, D., F. Sun, Z. Liu, Z. Cong, G. Ni, and Z. Lei (2007), Analyzing spatial and temporal variability of annual water-energy balance in nonhumid regions of China using the Budyko hypothesis, *Water Resour. Res.*, *43*, W04426, doi:10.1029/2006WR005224.

Yokoo, Y., M. Sivapalan, and T. Oki (2008), Investigation of the relative roles of climate seasonality and landscape properties on mean annual and monthly water balances, *J. Hydrol.*, *357*(3-4), 255–269, doi:10.1016/j.jhydrol.2008.05.010.

Zhang, L., W. R. Dawes, and G. R. Walker (2001), Response of mean annual evapotranspiration to vegetation changes at catchment scale, *Water Resour. Res.*, *37*, 701–708.

C. J. Harman, M. Sivapalan, and M. A. Yaeger, Department of Civil and Environmental Engineering, University of Illinois at Urbana-Champaign, Urbana, IL 61801, USA. (sivapala@illinois.edu)

P. A. Troch, Department of Hydrology and Water Resources, University of Arizona, John W. Harshbarger Bldg. Rm. 320A, Tucson, AZ 85721, USA.

X. Xu, Department of Geography, University of Illinois at Urbana-Champaign, Urbana, IL 61801, USA.